Draft version February 13, 2017
Preprint typeset using LaTeX style AASTeX6 v. 1.0

HW 02: INTRODUCTION TO STELLAR SPECTRA

Bryan Yamashiro[1]
University of Hawaii at Manoa
2500 Campus Road
Honolulu, HI 96822

1. INTRODUCTION

This study involved the use of both the Boltzmann and Saha Equations. The purpose of the exercises was to examine the hydrogen populations and the corresponding temperature dependences. An additional step is taken to observe the dependence on variant mass densities whilst invoking the Saha methodology.

The second part of the study was to become familiarized with stellar spectrum data. The spectrum data utilized for this study was wavelength-calibrated and also intensity-normalized. The data was provided in ascii format with wavelengths in nanometers in the first column, and normalized intensity in the second column. Further corrections were applied such as compensations for the heliocentric radial velocity, and those details were used to directly probe radial velocities.

2. BOLTZMANN AND SAHA EQUATIONS

The number density,(n_H) of H atoms at some point near the photosphere was found to be $1.259E40\,\mathrm{atoms/cm^3}$, using equation 1. The three variables include Avogadro's constant (N_A), the atomic mass of a hydrogen atom (M_H), and the mass density (ρ). Although the first two variables are constant, the latter mass density (ρ_1) was set to $3.5E{-}7\,\mathrm{g/cm^3}$. To represent the Saha equation dependence on mass density, the updated value (ρ_2) was lowered to $3.5E{-}8\,\mathrm{g/cm^3}$, and re-labeled in table 1.

$$n_H = \frac{N_A}{M_H}\rho \tag{1}$$

Table 1. Population results from Boltzmann and Saha Equations

Temperature [K]	Population (Boltzmann) [n_2/n_1]	Population (Saha [ρ_1]) [n_2/n_1]	Ratio of Population (Saha [ρ_2]) [n_2/n_1]
3000	5.678E-23	6.979E-25	6.979E-24
5000	7.822E-14	1.603E-15	1.603E-14
8000	1.082E-08	3.546E-10	3.546E-09
10000	5.594E-07	2.292E-08	2.292E-07

Note—All results from both the Boltzmann and Saha equations. Equations used to arrive to results are provided in source code in the appendix.

3. STELLAR SPECTRUM

The spectrum within the 4200 Å to 6200 Å, shown in figure 1, was probed to find the elements that corresponded to each absorption of the object. The spectrum included absorption line elements from hydrogen, oxygen, sodium, and iron. The sodium line at 5895.61 Å exhibited the largest absorption, followed by the hydrogen lines. The largest absorption features are included in table 2 (Hearnshaw (1986)).

Table 2. Absorption Line Elements in Spectrum

Wavelength [Å]	Designation	Element
6562.81	C (Hα)	H
6276.61	a	O_2
5895.61	D_2	Na
4861.34	F (Hβ)	H
4340.47	G' (Hγ)	H
4307.74	G	Fe

NOTE—The elements corresponding to each absorption line of the stellar spectrum and the respective element, designation, and wavelength.

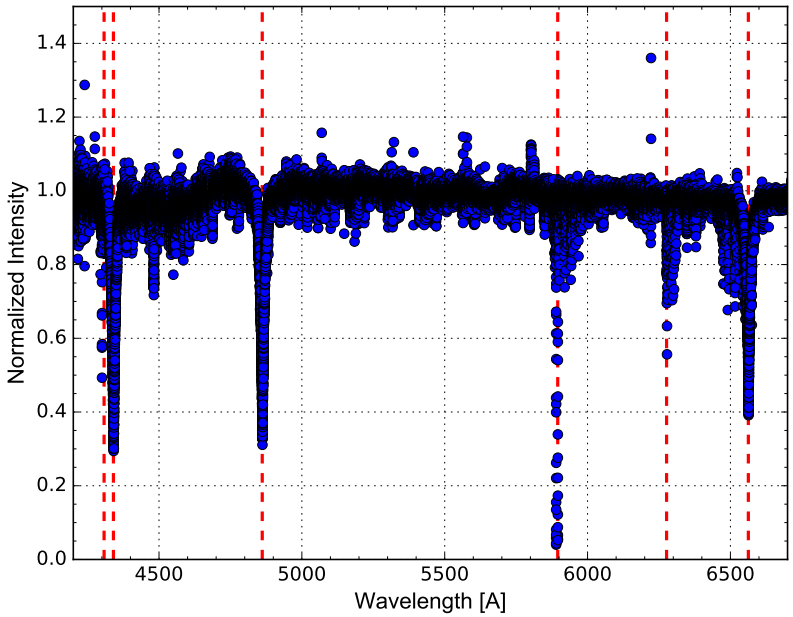

Figure 1. A full stellar spectrum from 4200 Å to 6200 Å. The largest absorption features were indicated with red dashed lines.

Along with the six elements included in this study, the radial velocities, provided in table 3, were also calculated. Radial velocity (V) calculations were conducted with the speed of light (c), the literature element peak wavelength (λ), and the shifted element peak wavelength ($\Delta\lambda$), shown in equation 2.

$$V = \frac{c\Delta\lambda}{\lambda} \tag{2}$$

Table 3. Elemental Absorptions in Spectrum

Element	Wavelength [Å]	Gaussian Peak [Å]	Radial Velocity [km/s]
Mg II	4481.228	4481.9	44.95654579
Fe II	4508.27	4508.97	46.54883594
N V	4603.73	4604.64	59.25871777
O V	5114.07	5115.09	59.7935318
C IV	5801.33	5802.42	56.32739031
C IV	5811.98	5813.1	57.77162911

NOTE—Elements with the literature wavelengths. The literature values were subtracted with the modulus of the measured intensity peaks for radial velocity measurements.

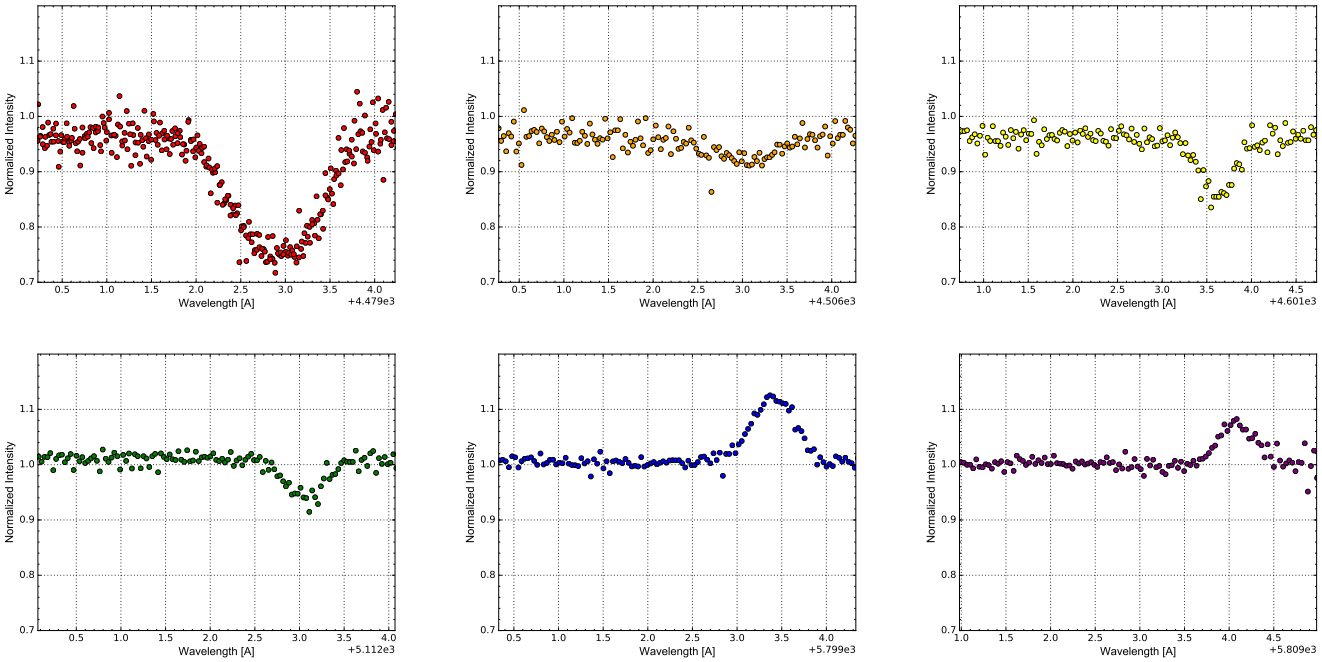

Figure 2. Spectral features for Mg II (red), Fe II (orange), N V (yellow), O V (green), C IV (blue), C IV (purple). As the intensities are normalized, positive or negative peak, relative to the background, shows absorption or emission traits.

Figure 3 (left) shows a Gaussian fit of the Mg II absorption feature. To compare to the instrumental profile, the Gaussian will be compared to the instrumental fit in equation 3. The full width at half-maximum in this case will be equal to λ/R. The variable λ will be the literature value for Mg II, 4481.228 Å. Additionally, the spectral resolution, R, of the Canada-France-Hawaii Telescope on Mauna Kea is 68000.

$$I(x) = \exp -\frac{x^2}{2\sigma^2} \tag{3}$$

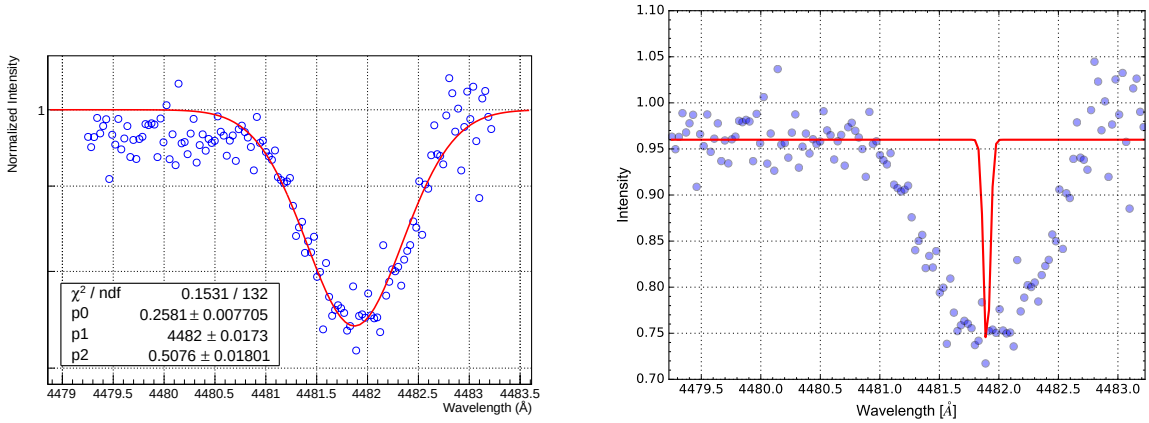

Figure 3. **Left:** stellar spectrum for Mg II is shown with a Gaussian fit. **Right:** The stellar spectrum for Mg II is shown with the instrumental profile.

Figure 3 (right) shows the less broadened spectra. It is clear that the FWHM in this scenario is far reduced compared to the fuller profile in figure 3. The most probable extra broadening could be attributed to "Macroscopic Doppler Broadening" for this object. Radial velocities included a discrepancy of more than 10 Å between the six elements, therefore there may exist a variable line-of-sight velocity of the object.

4. CONCLUSION

The Boltzmann and Saha equations showed that the population of the first exited state hydrogen atoms does increase with increasing temperatures. The slight discrepancy for the Saha equations when varying mass density by decreasing a magnitude, was an inverse relation of population increase by a magnitude.

The strongest absorptions of the provided stellar spectrum included hydrogen, oxygen, sodium, and iron. The most intense absorption was the sodium line followed closely by the hydrogen lines. Probing the six elements with the respective wavelengths yielded shifted intensity peak and correlating radial velocities.

Finally, the instrumental broadening is far less prominent than the actual Gaussian fit. This effect was concluded to be less broad due to Macroscopic Doppler Broadening due to the varying radial velocities shown.

5. ADDENDUM

Discerning between the two objects were quite trivial as hints to two different species first arose from the radial velocities. In table 3, Two of the spectral lines exhibit radial velocities near 45 km/s and the remainder exhibit velocities at approximately 57 km/s. Since the resolution of the telescope is very fine at 68000, the velocities would not be close within the margin of error. Secondly, another hint arises out of the difference in evolution. The Mg and Fe are both early types are type II's, whereas the N, O, and C are type IV's and V's. Due to the spectral line elemental features, these objects are most likely stars, as C-N-O is present in many late type stars, and Fe-Mg can also be produced in early types.

The two possibilities for the setup of these stars are possibly 1) a binary system or 2) an optical anomaly, being one star is much further away from the other.. The supporting claim is that the discrepancy in radial velocities means that they are of two differing objects. The second possibility is currently more probable due to the short time interval. To distinguish between the two possibilities, the radial velocities must be probed for the two objects for a longer period of time.

REFERENCES

Hearnshaw, J.B. (1986). The analysis of starlight. Cambridge:
Cambridge University Press. ISBN 0-521-39916-5.

6. APPENDIX

Source code for generating all data and plots will be provided in external files (hw2.py, flux.cpp).